STATISTICS, OPTIMIZATION AND INFORMATION COMPUTING
Stat., Optim. Inf. Comput., Vol. 15, February 2026, pp 1258–1267.
Published online in International Academic Press (www.IAPress.org)

Attention-Enhanced Deep Convolutional Denoising Autoencoder for Cervical Cancer Image Quality Improvement

Salma Oussahi[1,*], Aziz Darouichi [1], El Mahdi El Guarmah [1,2]

[1] L2IS, FST, Cadi Ayyad University, Marrakech, Morocco
[2] Royal Air School of Aeronautics, Mathematics and Informatics Department, Marrakech, Morocco

Abstract Cervical cancer remains a major global health challenge, where the reliability of Pap smear–based screening is often compromised by imaging artifacts such as noise, blur, and staining variability. To address this issue, we propose an Attention-Enhanced Deep Convolutional Denoising Autoencoder (AE-DCDA) that incorporates Convolutional Block Attention Modules (CBAM) within an encoder–decoder structure. This design enables the network to adaptively focus on diagnostically relevant cellular structures while suppressing heterogeneous noise patterns. The model is trained and evaluated on two benchmark cervical cytology datasets, Herlev (917 images) and SIPaKMeD (4,049 images), with added localized Gaussian noise to simulate realistic acquisition conditions. Experimental results demonstrate that AE-DCDA consistently outperforms conventional filters and competitive deep learning baselines such as DnCNN, FFDNet, and Noise2Void. Specifically, it achieves improvements exceeding 10 dB in PSNR on Herlev and over 4 dB on SIPaKMeD, while also reducing inference time. Visualization of attention maps further confirms that the model effectively highlights nuclei and cytoplasmic regions, thereby improving interpretability and diagnostic trustworthiness. These findings suggest that attention-augmented denoisers represent a promising direction for robust preprocessing in cervical cancer image analysis pipelines.

Keywords Cervical cancer, Pap-smear images, Image processing, Preprocessing, Deep learning, Autoencoder, Attention mechanism

AMS 2020 subject classifications 68T07, 68T45, 68U10

DOI: 10.19139/soic-2310-5070-2777

1. Introduction

Cervical cancer remains one of the leading causes of cancer-related deaths among women worldwide [1, 2]. Early detection is crucial for successful treatment, and Pap smear screening plays a key role in identifying precancerous and cancerous cells. However, manual examination of Pap smear slides is time-consuming, subjective, and often suffers from inter-observer variability, which can delay diagnosis and treatment.

During acquisition, cervical cytology images are frequently degraded by noise and artifacts caused by staining variations, motion blur, and imperfect imaging conditions. These degradations reduce image quality and impair downstream computer-aided diagnosis tasks such as segmentation and classification [3]. Traditional denoising methods, including Gaussian, Median, Wiener, and Bilateral filters, have been widely applied [4, 5, 6]. While they can improve peak signal-to-noise ratio (PSNR) and structural similarity index (SSIM) under specific conditions, their hand-crafted nature limits their ability to adaptively preserve fine diagnostic details, making them suboptimal for medical imaging applications.

*Correspondence to: Salma Oussahi (Email: s.oussahi.ced@uca.ac.ma). Department of Computer Science, FST, Cadi Ayyad University. Bd. Abdelkrim El Khattabi, B.P. 549 Guéliz, Marrakech (40000), Morocco.

ISSN 2310-5070 (online) ISSN 2311-004X (print)

In recent years, deep learning-based approaches have demonstrated superior performance in image restoration tasks. Convolutional neural network (CNN)-based denoisers such as DnCNN [7], FFDNet [8], Noise2Void [9] and denoising autoencoders [10] have shown remarkable capability in suppressing global noise while preserving structural details. However, cervical cytology images are often degraded by localized, non-uniform noise, arising from staining variations, debris, and acquisition artifacts. Conventional deep architectures tend to treat noise as spatially uniform, which limits their effectiveness in addressing such heterogeneous degradations. To overcome this, attention mechanisms—particularly channel and spatial attention—offer a principled way to adaptively highlight informative regions and suppress noisy or irrelevant background areas, thereby making denoising more robust to localized perturbations.

In this paper, we propose an Attention-Enhanced Deep Convolutional Denoising Autoencoder (AE-DCDA) designed specifically for improving the quality of cervical cytology images. The contributions of this work are summarized as follows:

- We introduce a novel autoencoder architecture enhanced with Convolutional Block Attention Modules (CBAM), allowing the model to selectively focus on important spatial and channel features to improve denoising performance.
- We conduct an extensive ablation study to isolate the contribution of the attention mechanism by comparing AE-DCDA with and without CBAM, evaluating both image quality metrics and computational efficiency.
- We validate the proposed model on two widely used cervical cytology datasets: the Herlev dataset (small-scale, 917 images) and the SIPaKMeD dataset (large-scale, 4,049 images). This dual evaluation demonstrates both robustness and generalizability.
- We provide visualization of the attention maps, highlighting how the model focuses on noisy regions and salient cellular structures, thereby improving interpretability and clinical trustworthiness.

The remainder of this paper is organized as follows. Section 2 reviews related work on traditional and deep learning-based denoising methods. Section 3 presents the proposed AE-DCDA model and its attention mechanism and an exploration of the datasets. Section 4 reports the quantitative and qualitative results on the Herlev and SIPaKMeD datasets, including ablation studies and attention map visualization. Section 5 discusses the key points of the experimental results. Finally, Section 6 concludes the paper and outlines future research directions.

2. Related Work

Traditional denoising techniques are widely used, and several studies have exploited them in cervical cytology image enhancement. [11] conducted a study that included classical filters such as Gaussian, Median, Wiener, Bilateral, and Local Laplacian filtering, which are generally designed to reduce Gaussian, speckle, or Poisson noise. Although they can achieve reasonable performance their effectiveness is fundamentally constrained by the hand-crafted nature of their operations. In [12], classical filters such as Blur, Bilateral, Median, Gaussian, and Blur Bilateral were applied to Pap smear images from the SIPaKMeD dataset and evaluated using a CNN-based decision support system (NasNetLarge). Among them, Gaussian blur produced the best results, outperforming other filters and the baseline model without enhancement. In [13], the median filter is employed as a preprocessing step to suppress noise and enhance image quality, thereby facilitating more accurate segmentation with K-Means and subsequent classification using the optimized MCNN. The detailed results of these traditional filters are summarized in Table 1. However, despite these results, filter-based methods remain limited, as they provide only marginal improvements and cannot adaptively distinguish between noise and subtle diagnostic features, thereby motivating the need for deep learning-based denoising strategies.

Table 1. Performance of traditional denoising techniques applied to cervical cytology images.

Study	Dataset	Noise / Task	Filters	Results / Metrics
[11]	Clinical dataset	Gaussian noise ($\sigma^2 = 0.01$)	Gaussian	PSNR ∼25–27, SSIM < 0.80
			Median	PSNR ∼26–28, SSIM ∼0.80
			Wiener	PSNR > 28, SSIM > 0.80
			Bilateral	PSNR > 28, SSIM > 0.80
			Local Laplacian	PSNR > 30, SSIM > 0.90
[12]	SIPaKMeD dataset	Pre-processing for CNN classification	Gaussian Blur	Enhanced accuracy = 86.79% Enhanced sensitivity = 86.81% Enhanced specificity = 96.70% Enhanced F1 = 86.78%
			Bilateral	Lower than Gaussian Blur
			Median	Lower than Gaussian Blur
			Blur Bilateral	Lower than Gaussian Blur

The study [14] introduces a structured deep learning framework designed to enhance image quality by systematically comparing state-of-the-art denoising models, including DnCNN, FFDNet, Noise2Noise, SwinIR, BM3D, and Non-Local Means. To simulate realistic acquisition conditions, the authors artificially introduced 40% Poisson noise into a dataset of 5,172 Pap smear images. The framework evaluates each denoising method both quantitatively, using PSNR, SSIM, SNR, and MSE and qualitatively, the results are reported in Table 2. Results demonstrate that deep learning-based methods consistently outperform traditional approaches, with SwinIR achieving the best overall performance. These findings highlight the ability of transformer-based models to preserve crucial morphological features while effectively suppressing noise, thereby improving the diagnostic reliability of Pap smear screening.

Table 2. Performance of denoising algorithms on Pap smear images corrupted with 40% Poisson noise.

Algorithm	SSIM	SNR	PSNR	MSE
DnCNN	0.89	20.5	28.7	0.001349
FFDNet	0.87	19.8	27.9	0.001622
Noise2Noise	0.88	20.0	28.1	0.001549
SwinIR	0.91	21.2	29.5	0.001122
BM3D	0.85	18.5	26.3	0.002344
Non-Local Means	0.82	17.8	25.7	0.002692

3. Proposed Methodology

3.1. Dataset Exploration

The Herlev dataset [15] contains 917 cervical cell images at 256×256 pixels. Each image is assigned to one of seven categories "Carcinoma in Situ", "Light Dysplastic", "Moderate Dysplastic", "Normal Columnar", "Normal Intermediate", "Normal Superficial", and "Severe Dysplastic" covering the progression from healthy cells through precancerous alterations to malignant stages. The specifics of this dataset are shown in Table 3. The dataset is suitable for classification, segmentation, and denoising tasks. The images were normalized to a range between 0 and 1, and local Gaussian noise was added to simulate real imaging conditions, which are often affected by artifacts. The corresponding images of these classes are shown in Figure 1.

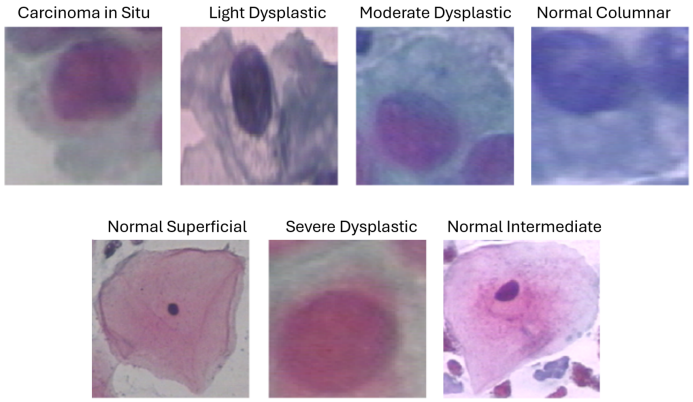

Figure 1. Sample images from the Herlev dataset representing seven distinct classes of cervical cells.

Table 3. Distribution of the Herlev dataset

Category	Type	Number of Cells
Normal Superficial	Normal	74
Normal Intermediate		70
Normal Columnar		98
Light Dysplasia	Abnormal	182
Moderate Dysplasia		146
Severe Dysplasia		197
Carcinoma in situ		150
Total		917

The SIPaKMeD dataset [16] consists of 4,049 cervical cell images acquired from Pap smear slides under more diverse and realistic laboratory conditions compared to Herlev. Each image has been carefully segmented and classified into five categories: Superficial-Intermediate, Parabasal, Koilocytotic, Dyskeratotic, and Metaplastic. The class distribution is detailed in Table 4. Unlike Herlev, which is relatively small and collected under controlled conditions, SIPaKMeD provides a larger and more diverse sample set, making it particularly suitable for validating the robustness and generalizability of denoising models. Representative samples are presented in Figure 2.

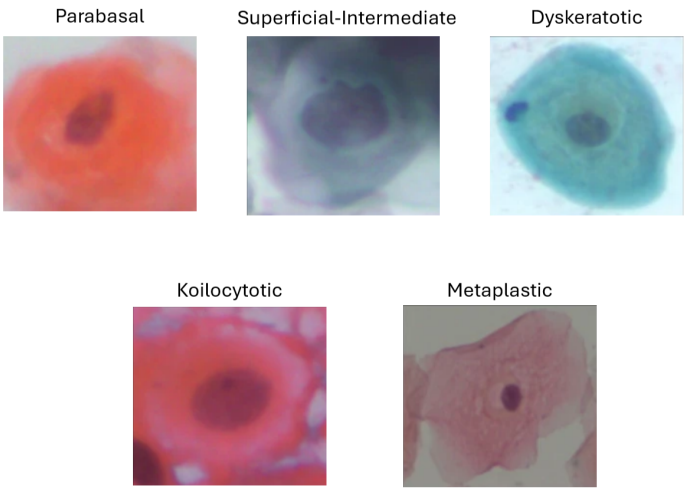

Figure 2. Sample images from the SIPaKMeD dataset representing five distinct cervical cell categories.

Table 4. Distribution of the SIPaKMeD dataset

Category	Number of Cells
Superficial-Intermediate	831
Parabasal	787
Koilocytotic	825
Dyskeratotic	813
Metaplastic	793
Total	4,049

3.2. Model Architecture

Our proposed model is an Attention-Enhanced Deep Convolutional Denoising Autoencoder (AE-DCDA) for denoising cervical cancer images, as illustrated in Figure 3. The encoder progressively down-samples the noisy input image through three convolutional blocks with 64, 128, and 256 filters, respectively. A bottleneck layer with 512 filters acts as a compressed latent representation, preserving essential structures while suppressing noise. Attention mechanisms (CBAM: Channel and Spatial Attention) [17]

are applied after the first and second encoder blocks, allowing the model to emphasize informative features by generating attention maps. The decoder mirrors the encoder with transposed convolutional layers, gradually upsampling the latent features back to the original resolution. Skip connections are employed by concatenating decoder features with the refined outputs from the attention blocks, ensuring effective feature reuse and better gradient flow. Finally, a convolutional layer with a sigmoid activation reconstructs the denoised image. This attention-enhanced strategy enables the network to selectively focus on salient regions, thereby improving denoising performance. To balance pixel-level fidelity and structural preservation, we adopted a hybrid loss function combining Mean Squared Error (MSE) and Structural Similarity (SSIM) loss as formulated in Equation (1):

$$\mathcal{L}_{\text{MSE}} = \frac{1}{N}\sum_{i=1}^{N}(\hat{x}_i - x_i)^2 \quad ; \quad \mathcal{L}_{\text{SSIM}} = 1 - SSIM(\hat{x}, x) \quad ; \quad \mathcal{L}_{\text{total}} = \mathcal{L}_{\text{MSE}} + \lambda \cdot \mathcal{L}_{\text{SSIM}} \tag{1}$$

with $\lambda = 0.05$ in our experiments. This formulation mitigates the over-smoothing effect of pure MSE loss while preserving the morphological structures of cervical cells.

3.3. Attention Mechanism Formulation

To enhance the denoising capability of the proposed AE-DCDA, we integrate Convolutional Block Attention Modules (CBAM) after the first and second encoder stages. CBAM combines both channel and spatial attention to refine the extracted features. Below, we provide the mathematical formulation.

3.3.1. Channel Attention: Given an intermediate feature map $\mathbf{F} \in \mathbb{R}^{C\times H\times W}$, channel attention exploits both global average pooling and global max pooling to aggregate spatial information into channel descriptors:

$$\mathbf{f}^c_{avg} = \text{GAP}(\mathbf{F}), \quad \mathbf{f}^c_{max} = \text{GMP}(\mathbf{F}), \tag{2}$$

where $\mathbf{f}^c_{avg}, \mathbf{f}^c_{max} \in \mathbb{R}^{C\times 1\times 1}$. These descriptors are passed through a shared multi-layer perceptron (MLP) with a reduction ratio r to model inter-channel dependencies:

$$\mathbf{M}_c(\mathbf{F}) = \sigma\big(W_2(\delta(W_1\mathbf{f}^c_{avg})) + W_2(\delta(W_1\mathbf{f}^c_{max}))\big), \tag{3}$$

where $W_1 \in \mathbb{R}^{C/r\times C}$, $W_2 \in \mathbb{R}^{C\times C/r}$ are learnable weights, $\delta(\cdot)$ is the ReLU activation, and $\sigma(\cdot)$ is the sigmoid function. The channel-refined feature map is obtained as:

$$\mathbf{F}' = \mathbf{M}_c(\mathbf{F}) \otimes \mathbf{F}, \tag{4}$$

where $\otimes$ denotes channel-wise multiplication.

3.3.2. Spatial Attention: To focus on informative regions, channel-refined features $\mathbf{F}'$ are further processed with spatial attention. First, spatial descriptors are computed via channel-wise average pooling and max pooling:

$$\mathbf{f}^s_{avg} = \frac{1}{C}\sum_{i=1}^{C}\mathbf{F}'_i, \quad \mathbf{f}^s_{max} = \max_{i\in[1,C]}\mathbf{F}'_i, \tag{5}$$

where $\mathbf{f}^s_{avg}, \mathbf{f}^s_{max} \in \mathbb{R}^{1\times H\times W}$. These are concatenated and convolved with a $k\times k$ kernel (we set $k = 7$):

$$\mathbf{M}_s(\mathbf{F}') = \sigma\big(f^{k\times k}([\mathbf{f}^s_{avg}; \mathbf{f}^s_{max}])\big). \tag{6}$$

The final spatially refined features are:

$$\mathbf{F}'' = \mathbf{M}_s(\mathbf{F}') \otimes \mathbf{F}'. \tag{7}$$

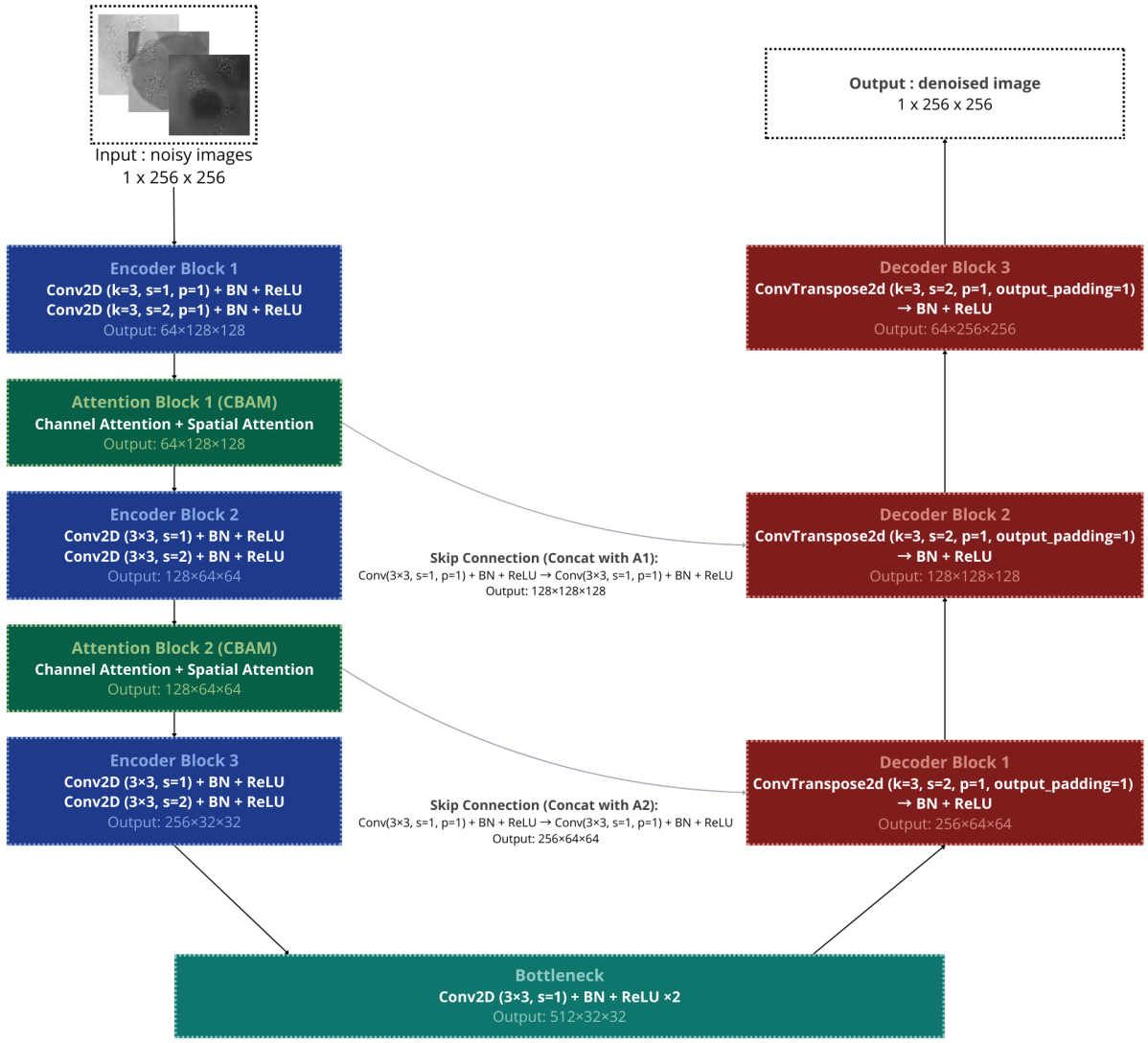

Figure 3. Proposed AE-DCDA architecture: an encoder–decoder with CBAM attention and skip connections.

3.3.3. Integration with the Decoder: The refined features $\mathbf{F}''$ are propagated through skip connections and concatenated with the corresponding decoder outputs to improve reconstruction. The attention maps $\mathbf{M}_c$ and $\mathbf{M}_s$ act as scaling operators, emphasizing salient information while suppressing irrelevant noise.

3.4. Evaluation Metrics

To evaluate the performance of the proposed AE-DCDA model, we employ widely used image quality assessment metrics:

- Peak Signal-to-Noise Ratio (PSNR): Measures the ratio between the maximum possible signal power and the power of corrupting noise, expressed in decibels (dB). Higher PSNR indicates better denoising quality.

- Structural Similarity Index (SSIM): Assesses the structural fidelity between the denoised image and the ground truth, with values ranging from 0 to 1. A higher SSIM reflects better preservation of structural information.
- Inference Latency / FPS: Measures the average processing time per image and the corresponding throughput in frames per second (FPS), reflecting the model's suitability for deployment in clinical workflows.

3.5. Uncertainty Quantification with Monte Carlo Dropout

To further assess the robustness of the proposed AE-DCDA model, we incorporate Monte Carlo (MC) Dropout as a practical method for uncertainty quantification. Unlike standard inference where dropout layers are disabled, MC Dropout keeps them active at test time and performs multiple stochastic forward passes for the same input image. By aggregating the outputs across T passes, the model yields both a mean prediction (improving stability) and a pixel-wise variance map that reflects prediction confidence. This approach provides reliable confidence intervals for metrics such as PSNR and SSIM, offering additional insight into the reliability of the model in high-stakes diagnostic applications.

4. Experimental Results

To further validate the effectiveness and generalization of the proposed AE-DCDA model, we conducted experiments on two cervical cytology datasets of different scales: the larger SIPaKMeD dataset and the smaller Herlev dataset (917 images). For both datasets, we performed an ablation study by training the autoencoder with and without attention blocks. Quantitative results are reported in Tables 5 and 6, while qualitative comparisons are illustrated in Figures 4 and 6. The visualization of attention maps in Figures 5 and 7 further highlights how the first attention block (Att1) captures localized noisy patches, while the second (Att2) emphasizes global structural patterns. Across both datasets, the CBAM-enhanced variant consistently outperforms the baseline, achieving over 10 dB improvement in PSNR on the Herlev dataset and notable gains in SSIM, while also reducing inference time. These results demonstrate that the proposed design not only enhances denoising quality but also improves computational efficiency, even under limited data conditions. Moreover, on the SIPaKMeD dataset, we additionally trained three representative denoising baselines—DnCNN, FFDNet, and Noise2Void (N2V)—under exactly the same experimental conditions, including identical train/validation/test splits, 256×256 resolution inputs, and the same evaluation metrics (PSNR, SSIM, Inference Time, Parameter Count (Params), and Model Size (Size)). Finally, to assess the robustness and reliability of the proposed approach in high-stakes diagnostic contexts, we conducted uncertainty quantification using Monte Carlo Dropout ($T = 20$ stochastic passes). The CBAM-enhanced AE-DCDA achieved a mean PSNR of 42.59 dB [42.55 – 42.63] and SSIM of 0.979 [0.979 – 0.980] (95% confidence interval), while the non-attention variant reached 36.29 dB [36.26 – 36.32] and 0.963 [0.963 – 0.964], respectively. Moreover, the pixel-wise uncertainty standard deviation was lower for the CBAM variant (≈ 0.006) compared to the baseline (≈ 0.007), confirming that attention not only improves average performance but also strengthens the model's confidence in its predictions.

Table 5. Ablation study on the effect of the attention mechanism (CBAM) in the AE-DCDA model, evaluated on the SIPaKMeD dataset.

Model	PSNR (dB)	SSIM	Inference Time (ms)	FPS	Params (M)	Size (MB)
AE-DCDA (No-Att)	38.244	0.9740	9.013	110.95	8.084	30.862
AE-DCDA (CBAM)	42.594	0.9794	7.049	141.86	8.081	30.851
DnCNN	28.850	0.7819	9.46	105.7	0.56	6.45
FFDNet	39.31	0.963	1.58	634.1	0.38	1.44
N2V	41.59	0.970	2.28	439.5	0.47	1.78

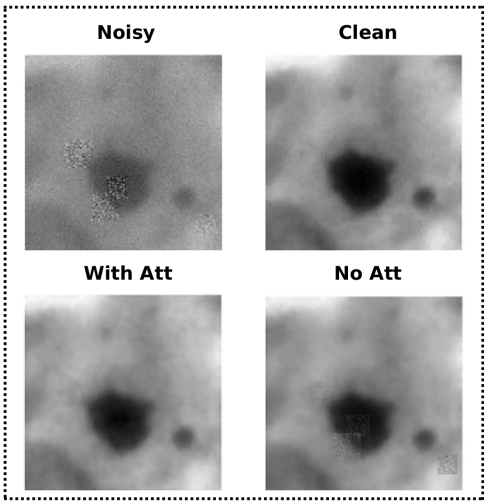

Figure 4. Qualitative comparison of denoising performance with and without the attention mechanism on the SIPaKMeD dataset.

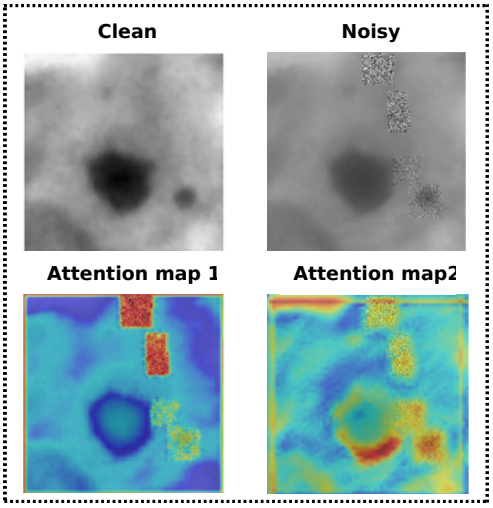

Figure 5. Visualization of the attention maps generated by the AE-DCDA model on the SIPaKMeD dataset.

Table 6. Ablation study on the effect of the attention mechanism (CBAM) in the AE-DCDA model, evaluated on the Herlev dataset.

Model	PSNR (dB)	SSIM	Inference Time (ms)	FPS	Params (M)	Size (MB)
AE-DCDA (No-Att)	28.611	0.9404	9.013	110.95	8.084	30.862
AE-DCDA (CBAM)	38.863	0.9577	7.049	141.86	8.081	30.851

5. Discussion

The experimental results provide several important insights. First, the ablation on both SIPaKMeD and Herlev datasets confirms that the inclusion of CBAM attention modules substantially improves denoising quality. The gains are consistent across metrics: PSNR improves by more than 4 dB on SIPaKMeD and by over 10 dB on Herlev, while SSIM is also enhanced. The qualitative visualizations further validate that the attention mechanism effectively identifies localized noise patterns and preserves global structural information. This dual capability explains why the CBAM-enhanced variant consistently outperforms the baseline autoencoder. Second, the comparative evaluation against well-established denoising networks highlights the efficiency of the proposed design. Although DnCNN remains lightweight, its reconstruction quality is clearly insufficient for cytology images, confirming the necessity of more advanced architectures. FFDNet achieves the fastest inference time and smallest memory footprint, which is advantageous for real-time deployment, but its PSNR and SSIM remain lower than the proposed model. Noise2Void provides competitive results without requiring clean labels, but its self-supervised nature still falls short of the attention-augmented AE-DCDA. These findings suggest that attention not only improves representational capacity but also leads to more favorable trade-offs between accuracy and efficiency. Third, the results on the small Herlev dataset demonstrate the robustness of the model under data scarcity. In many biomedical contexts, collecting large amounts of high-quality annotated data is challenging. The significant improvement on Herlev suggests that attention-based designs are less prone to overfitting and can generalize better in low-data regimes, which is critical for real-world clinical applications.

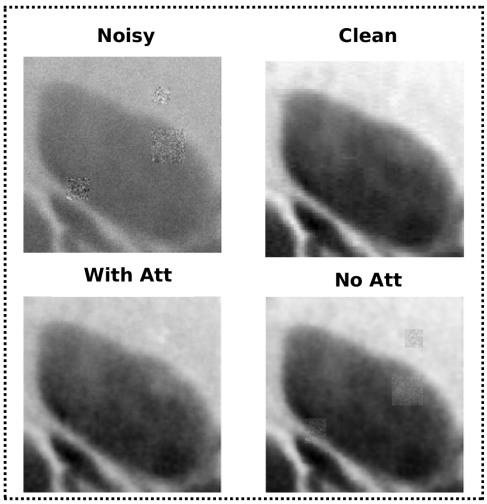

Figure 6. Qualitative comparison of denoising performance with and without the attention mechanism on the Herlev dataset.

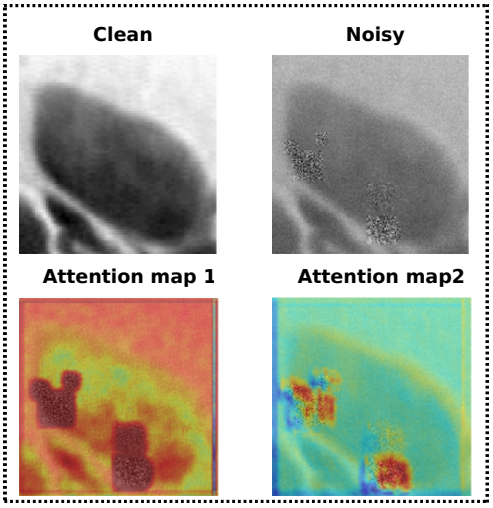

Figure 7. Visualization of the attention maps generated by the AE-DCDA model on the Herlev dataset.

6. Conclusion and Future Work

In this paper, we presented an Attention-Enhanced Deep Convolutional Denoising Autoencoder (AE-DCDA) specifically tailored for improving the quality of cervical cytology images. By integrating channel and spatial attention through CBAM modules, the proposed framework successfully addresses the challenge of non-uniform noise while preserving crucial diagnostic details. Experimental evaluations on both the Herlev and SIPaKMeD datasets demonstrated substantial improvements in PSNR and SSIM compared with both traditional filters and well-established deep learning denoisers such as DnCNN, FFDNet, and Noise2Void. Beyond quantitative gains, qualitative visualizations of attention maps confirmed the interpretability and robustness of the approach, showing that the model adaptively emphasizes nuclei and cytoplasmic boundaries while suppressing artifacts. These results highlight two key insights. First, attention mechanisms significantly enhance denoising performance and generalization, even under limited training data conditions. Second, the balance achieved between accuracy and computational efficiency suggests strong potential for integration into real-world computer-aided diagnosis workflows. Future work will focus on extending AE-DCDA to multi-modal imaging scenarios such as cervigrams and MRI, and on integrating the denoising framework into downstream tasks including segmentation and classification to further support comprehensive cervical cancer diagnosis.

REFERENCES

1. International Agency for Research on Cancer. Cancer today. https://gco.iarc.who.int/today/, 2022.
2. World Health Organization. https://www.who.int/health-topics/cervical-cancer#tab=tab_1, 2022.
3. Salma Oussahi, Aziz Darouichi, and El Mahdi El Guarmah. Segmentation of cervical cancer from mri images: An overview. In 2024 International Conference on Connected Innovation and Technology (ICCITX), pages 1–6, 2024.
4. Veni N and Manjula J. Gaussian denoising by time domain and frequency domain filters for mri brain images. In 2022 IEEE IAS Global Conference on Emerging Technologies (GlobConET), pages 817–821, 2022.
5. Ginu George, Rinoy Mathew Oommen, Shani Shelly, Stephie Sara Philipose, and Ann Mary Varghese. A survey on various median filtering techniques for removal of impulse noise from digital image. In 2018 Conference on Emerging Devices and Smart Systems (ICEDSS), pages 235–238, 2018.
6. Amanpreet Kaur Sandhu and Jaskaran Singh Bhullar. Adaptive hybrid bilateral filter for efficient image denoising in noisy environments. In 2025 8th International Conference on Computing Methodologies and Communication (ICCMC),

pages 1574–1579, 2025.
7. Kai Zhang, Wangmeng Zuo, Yunjin Chen, Deyu Meng, and Lei Zhang. Beyond a Gaussian denoiser: Residual learning of deep CNN for image denoising. IEEE Transactions on Image Processing, 26(7):3142–3155, 2017.
8. Kai Zhang, Wangmeng Zuo, and Lei Zhang. Ffdnet: Toward a fast and flexible solution for cnn-based image denoising. IEEE Transactions on Image Processing, 27(9):4608–4622, 2018.
9. Alexander Krull, Tim-Oliver Buchholz, and Florian Jug. Noise2void - learning denoising from single noisy images. pages 2124–2132, 2019.
10. Woong Hee Lee, Mustafa Ozger, Ursula Challita, and Ki Won Sung. Noise learning-based denoising autoencoder. IEEE Communications Letters, 25(9):2983–2987, September 2021. Publisher Copyright: © 1997-2012 IEEE.
11. Maryza Intan Rahmawati, Siti Marhainis Binti Othman, Siti Nurul Aqmariah Mohd Kanafiah, Yessi Jusman, Anani Aila Mat Zin, and Nur Syuhada Mohd Nafis. Enhanced denoising of cervical pre-cancerous cell images through advanced color filtering. In 2024 4th International Conference of Science and Information Technology in Smart Administration (ICSINTESA), pages 317–322, 2024.
12. Ferat Efil and Zafer Cömert. Filter-based image enhancement effects on cnn-based decision support system for cervical cancer diagnosis. In 2024 8th International Symposium on Multidisciplinary Studies and Innovative Technologies (ISMSIT), pages 1–4, 2024.
13. S. Maheswari, C.N. Marimuthu, and Xavier N. Fernando. A robust automated cervical cancer detection system using Elephant Herding Optimized MCNN. 2025.
14. Nahida Nazir, Abid Sarwar, and Baljit Singh Saini. PAP-Net: A systematic framework for denoising pap smear images. SN Computer Science, 6(5):468, May 2025.
15. Yuvrajsinha Chowdhury. Herlev dataset, 2021.
16. Marina E. Plissiti, P. Dimitrakopoulos, G. Sfikas, Christophoros Nikou, O. Krikoni, and A. Charchanti. Sipakmed: A new dataset for feature and image based classification of normal and pathological cervical cells in pap smear images. In 2018 25th IEEE International Conference on Image Processing (ICIP), pages 3144–3148, 2018.
17. Sanghyun Woo, Jongchan Park, Joon-Young Lee, and In So Kweon. Cbam: Convolutional block attention module. In Vittorio Ferrari, Martial Hebert, Cristian Sminchisescu, and Yair Weiss, editors, Computer Vision – ECCV 2018, pages 3–19, Cham, 2018. Springer International Publishing.